

High resolution leaf wax carbon and hydrogen isotopic record of late Holocene paleoclimate in arid Central Asia

B. Aichner^{1,2}, S.J. Feakins¹, J.E. Lee³, U. Herzschuh^{4,2}, and X. Liu⁵

[1]{University of Southern California, Los Angeles, USA}

[2]{University of Potsdam, Potsdam, Germany}

[3]{Brown University, Providence, USA}

[4]{Alfred-Wegener-Institute, Potsdam, Germany}

[5]{Capital Normal University, Beijing, PR China}

Correspondence to: B. Aichner (bernhard.aichner@gmx.de)

Abstract

Central Asia is located at the confluence of large scale atmospheric circulation systems. It is thus likely to be highly susceptible to changes in the dynamics of those systems, however little is still known about the regions paleoclimate history. Here we present carbon and hydrogen isotopic compositions of *n*-alkanoic acids from a late Holocene sediment core from Lake Karakuli (eastern Pamir, Xinjiang Province, China). Instrumental evidence and isotope-enabled climate model experiments with the Laboratoire de Météorologie Dynamique Zoom model version 4 (LMDZ4) demonstrate that δD values of precipitation in the region are influenced by both temperature and precipitation amount. We find that those parameters are inversely correlated on an annual scale; i.e. climate varies between cool/wet and dry/warm over the last 50 years. Since the isotopic signals of these changes are in the same direction and therefore additive, isotopes in precipitation are sensitive recorders of climatic changes in the region. Additionally, we infer that plants are using year round precipitation (including snow-melt) and thus leaf wax δD values must also respond to shifts in the proportion of moisture derived from westerly storms during late winter/early spring. Downcore results give evidence for a gradual shift to cooler and wetter climates between 3.5 and 2.5 cal kyr BP, interrupted by a warm/dry episode between 3.0–2.7 kyr BP. Further cool and wet episodes occur between 1.9–1.5 kyr BP and between 0.6–0.1 kyr BP, the latter coeval with the Little Ice Age. Warm and dry episodes between 2.5–1.9 kyr BP and 1.5–0.6 kyr BP coincide with the Roman Warm Period and Medieval Climate Anomaly, respectively. Finally, we find a drying trend in recent decades. Regional comparisons lead us to infer that the strength and position of the Westerlies, and wider Northern Hemispheric climate dynamics control climatic

1 shifts in arid Central Asia, leading to complex local responses. Our new archive from Lake
2 Karakuli provides a detailed record of the local signatures of these climate transitions in the
3 eastern Pamir.

4
5 Keywords: Pamir, Tibetan Plateau; Muztagh Ata, paleolimnology; biomarker; climate model;
6 LMDZ4

8 **1 Introduction**

9 Future climate change associated with anthropogenic disturbance of the Earth system is
10 expected to go in hand with changes in atmospheric circulation dynamics (Seth et al., 2011).
11 In this scenario, certain regions of the Earth are thought to be susceptible to severe and likely
12 abrupt changes in moisture delivery and temperature. One such region is Central Asia, located
13 at the boundaries of influences from the mid-latitude Westerlies, the Siberian High, and the
14 limits of the Indian Monsoon (Aizen et al., 2001; Chen et al., 2008). However, the nature and
15 magnitude of changes in these climatic systems, as well as their Central Asian regional effects
16 are still poorly known. Detailed knowledge about past, naturally-driven climatic variability in
17 this region can contribute to a better understanding of the complex atmospheric circulation
18 system, which can in turn help to better predict possible impacts of future anthropogenically-
19 driven climate changes.

20 While a large number of studies have analysed climate dynamics in monsoonal eastern Asia
21 and the north- and southeastern Tibetan Plateau (e.g. reviewed in Morill et al., 2003, An et al.,
22 2006 and Herzschuh, 2006), the density of paleoclimate records in continental Central Asia
23 remains comparably low. Central Asian records include studies of glacial extent in the Pamir
24 (e.g. Narama, 2002a and b) and tree-ring width reconstructions (e.g. Esper et al., 2002;
25 Treydte et al, 2006). Lacustrine sedimentary archives exist from Kyrgyzstan (Ricketts et al.,
26 2001; Lauterbach et al., 2014, Mathis et al., 2014), the Aral Sea (Sorrell et al., 2007a and b;
27 Boomer et al., 2009; Huang et al., 2011), the Western and Southern Tarim Basin (Zhao et al.,
28 2012; Zhong et al., 2007), and the Pamirs/Tajikistan (Mischke et al. 2010c; Lei et al., 2014)
29 (Fig 1b). Only one of those studies has included compound specific hydrogen isotopic
30 analyses (Lauterbach et al., 2014), which have elsewhere in Asia shown potential to provide
31 information about moisture sources, precipitation amount and temperature (Mügler et al.;
32 2010, Aichner et al., 2010c; Liu et al., 2008).

1 Climatic patterns in Central Asia are complex due to the location on the boundary between
2 various large-scale atmospheric circulation systems, as well as the varied topography of the
3 area (Fig 1). While the easternmost parts are generally arid and receive most of their
4 precipitation during the summer, western regions receive higher proportional input from
5 Westerly-derived winter precipitation (Miehe et al., 2001; Machalett et al., 2008; Lauterbach
6 et al., 2014). Thus a dense network of paleoclimatic records is required to fully understand
7 spatial patterns of climate dynamics over time.

8 To further decipher past climatic processes in our study we generated a high-resolution, mid
9 to late Holocene paleoclimatic record from Lake Karakuli (western China), located in the
10 eastern Pamir mountain range, at the very westernmost edge of the Tibetan Plateau. Building
11 upon the work of Liu et al., (2014) who inferred glacial fluctuations from grain-size
12 parameters and elemental composition at the same lake, we use compound-specific carbon
13 ($\delta^{13}\text{C}$) and hydrogen (δD) isotopic compositions of long-chain ($>\text{C}_{24}$) *n*-alkanoic acids
14 originating from plant leaf waxes to deduce past climatic changes in our study area. To
15 evaluate the hydrogen isotopic data it is essential to understand what drives the variability of
16 the isotopic signal which is recorded by the biomarker in a specific study area. Therefore we
17 draw comparisons to isotope-enabled model experiments using the Laboratoire de
18 Météorologie Dynamique Zoom model version 4 (LMDZ4) simulations (Hourdin et al., 2006;
19 Risi et al., 2010; Risi et al., 2012a and b; Lee et al., 2012). On basis of this data we
20 characterize the processes controlling isotopic composition of precipitation over Central Asia
21 and discuss the implications for the interpretation of the biomarker isotopic evidence.

22

23 **2 Study site**

24 Lake Karakuli (also: Lake Kala Kule) is a small lake (ca. 1 x 1.5km) located at the
25 westernmost edge of Xinjiang Province (PR China) at an altitude of 3650 m, between the
26 massifs of Kongur Shan and Muztagh Ata, both exceeding 7500 m (Fig. 1a). Those mountains
27 which form the eastern edge of the Pamir plateau and the very westernmost edge of the
28 Tibetan Plateau are directly adjacent to the mountain ranges of Karakorum and Tien Shan.
29 The climate in this high altitude region is cold and dry. At Taxkorgan climate station, 80 km
30 south of Lake Karakuli (3090 m), average annual temperatures and precipitation amounts are
31 3.2°C and 69 mm, respectively (1957-1990; Miehe et al., 2001) with June and July being the
32 wettest months. Climatic data from Bulun Kul (3310 m), 30 km north of our study area, are in
33 a similar range (0.6 °C and 127 mm) with a precipitation maximum during spring and summer

1 (1956-1968; Miehe et al., 2001). At higher altitudes, precipitation amounts increase by
2 orographic forcing. At the Muztagh Ata, annual rain- and snowfall was estimated to account
3 for about 300 mm at the glacier accumulation zone (at 5919 m; Seong et al., 2009a) while
4 other studies estimated a water equivalent depth of 605 mm for snow accumulation at 7010 m
5 (Wu et al., 2008).

6 Lake Karakuli is an open freshwater lake with a maximum depth of 20 m. The relatively small
7 catchment comprises meltwater mainly derived from glaciers on the western flank of Mt.
8 Muztagh Ata. Those form an alluvial fan with several creeks which discharge into the lake
9 from the south while the single outflow drains towards the north (see Fig. 1 and Fig. S1).
10 Most of the glacial runoff derived from the surrounding massifs incl. the main glacier of
11 Muztagh Ata and Mt Kongur Shan does currently not discharge into the lake.

12 The sparse vegetation consists of alpine grasslands, partly used for pasture (see Fig S1), with
13 alpine desert at higher altitudes. Above 5500 m the landscape is fully glaciated (with valley
14 glaciers descending to 4300 m; Tian et al., 2006). Compared to other shallow lakes on the
15 Tibetan Plateau where macrophytes are numerous (Aichner et al., 2010b), there are only a few
16 emergent and submerged macrophytes on or close to the shores, and few indications for
17 submerged plants in the deeper parts of the lake.

18

19 **3 Material and methods**

20 **3.1 Coring and chronology**

21 A sediment core with a composite length of ca. 820 cm was taken in September 2008 at
22 38.43968 °N and 75.05725 °E from a water depth of 16 m, using an UWITEC coring system
23 and a floating platform (the coring position is shown in supplement S7). The chronology was
24 based-on seventeen radiocarbon ages derived from ^{14}C AMS dating conducted on total
25 organic carbon (TOC) (Liu et al., 2014). The 0 cal. yr BP (1950 A.D.) was derived from
26 $^{210}\text{Pb}/^{137}\text{Cs}$ dating and appeared at ca. 10.5 cm depth. A reservoir-effect of 1880 years was
27 extrapolated from dating of core-top samples and assumed to be constant throughout the core.
28 The ^{14}C -ages indicate a nearly constant sedimentation rate across 4.3 kyr. For calibration of
29 the ages and construction of the age-depth model the IntCal09 dataset was used (Reimer et al.,
30 2009) applying a Bayesian method (Blaauw and Christen, 2011); for details see Liu et al.
31 (2014).

1 **3.2 Lab chemistry**

2 Sediments were extracted with Accelerated Solvent Extraction system (ASE 350; Dionex),
3 under high pressure (1500psi) and temperature (100°C) and using DCM/MeOH (9:1) as
4 solvent. Alkanoic acids were separated from the total lipid extract using column
5 chromatography (5 cm x 40 mm Pasteur pipette, NH₂ sepra bulk packing, 60 Å), eluting with
6 2:1 DCM/isopropanol, followed by 4% formic acid in diethylether, yielding neutral and acid
7 fractions respectively. The acid fraction was esterified with 5% HCl and 95% methanol (of
8 known isotopic composition) at 70°C for 12 h to yield corresponding fatty acid methyl esters
9 (FAMES). Lipids were obtained by liquid-liquid extraction using hexane as the non-polar
10 solvent, and dried by passing through a column of anhydrous Na₂SO₄. They were further
11 purified using column chromatography (5 cm x 40 mm Pasteur pipette, 5% water-deactivated
12 silica gel, 100–200 mesh), eluting with hexane, followed by FAMES eluted with DCM.

13 **3.3 Biomarker isotopic analysis**

14 Compound specific isotopic values were obtained using gas chromatography isotope ratio
15 mass spectrometry (GC-IRMS). We used a Thermo Scientific® Trace gas chromatograph
16 equipped with a Rxi-5ms column (30 m x 0.25 mm, film thickness 1µm) and a programmable
17 temperature vaporizing (PTV) injector operated in solvent split mode with an evaporation
18 temperature of 60°C. The GC was connected via a GC Isolink with pyrolysis/combustion
19 furnace (at 1400/1000 °C) and a Conflo IV interface to a DeltaV_{plus} isotope ratio mass
20 spectrometer. The H₃⁺-factor (Sessions et al., 2001) was determined daily to test
21 measurement-linearity of the system and accounted for 5.8 ppm mv⁻¹ on average. Reference
22 peaks of H₂/CO₂ bracket *n*-alkanoic acid peaks during the course of a GC-IRMS run; two of
23 these peaks were used for standardization of the isotopic analysis, while the remainders were
24 treated as unknowns to assess precision. Except for the case of co-elution, precision of these
25 replicates was better than 0.6‰.

26 Data were normalized to the Vienna Standard Mean Ocean Water (VSMOW)-Standard Light
27 Antarctic Precipitation (SLAP) hydrogen isotopic scale and to Vienna Pee Dee Belemnite
28 (VPBD) carbon isotopic scale by comparing with an external standard containing 15 *n*-alkane
29 compounds (C₁₆ to C₃₀) of known isotopic composition (obtained from A. Schimmelmann,
30 Indiana University, Bloomington). The RMS error of replicate measurements of the standard
31 across the course of analyses was below 5‰ (hydrogen) and 0.7‰ (carbon) For hydrogen
32 isotopes we further monitored for instrument drift by measuring the δD values of a C₃₄ *n*-

1 alkane internal standard co-injected with the sample ($-240.6 \pm 3.0\%$; $n=105$). The isotopic
2 composition of H and C added during methylation of alkanolic acids was estimated by
3 methylating and analyzing phthalic acid as a dimethyl ester (isotopic standard from A.
4 Schimmelmann, University of Indiana) yielding $\delta D_{\text{methanol}} = -198.3 \pm 3.9\%$, $\delta^{13}C_{\text{methanol}} = -$
5 $25.45 \pm 0.42\%$ ($n=7$). Correction for H and C added by methylation was then made by way of
6 mass balance.

7 **3.4 LMDZ4 simulations**

8 To understand the control of spatial and seasonal isotopic variations, we use the climate
9 model LMDZ4 (Hourdin et al., 2006) to characterize the processes controlling isotopes of
10 precipitation over our study area. Details about the model and methodology are described in
11 Risi et al., (2010; 2012a and b) and Lee et al., (2012). Briefly, the applied model version
12 incorporates the entire cycle of stable water isotopes and includes fractionation when phase
13 changes occur. The resolution of the model is $2.5^\circ \times 3.75^\circ$ with 19 vertical levels in the
14 atmosphere. To obtain more realistic simulations of the hydrology and isotope values
15 compared with free-running simulations and to better reproduce the observed circulation
16 pattern, simulated winds from LMDZ4 are relaxed toward the pseudo-observed horizontal
17 wind field from the ERA-40 reanalysis results (Uppala et al., 2005) with a time constant of 1
18 hour. Boundary conditions used observed sea surface temperatures and sea ice fractions from
19 the HadISST data set (Rayner et al., 2003) from 1958 to 2009.

20

21 **4 Results**

22 **4.1 Lipid concentrations**

23 Due to the sparse vegetation in and around the lake, concentrations of leaf wax biomarkers in
24 the sediments were relatively low. For compound-specific isotopic analysis we chose fatty
25 acids (FAs) which showed higher concentrations than alkanes in a set of test samples. Here,
26 C_{24} , C_{26} and C_{28} *n*-alkanoic acids were the most abundant compounds, which average
27 concentrations of ca 1050, 1000 and 750 ng/g dw (nanograms per grams dry weight; Fig. S2).
28 We found fatty acid concentrations were relatively constant with depth, suggesting no major
29 change in productivity, dilution or preservation during the late Holocene.

30 **4.2 δD and $\delta^{13}C$ values of leaf wax lipids and water samples**

1 In total, we measured 125 core samples for hydrogen isotopic composition and 66 samples for
2 carbon isotopic composition (Tables S6). Samples contained C₁₆- C₂₈ *n*-alkanoic acids with an
3 even:odd chain length preference. We report isotopic results for the C₂₄, C₂₆ and C₂₈ *n*-
4 alkanolic acids as these are target long chain compounds within the dynamic range of isotopic
5 measurement capabilities (Tables S6, Fig. S3).

6 $\delta^{13}\text{C}$ values are generally more depleted with increasing chain-length, with C₂₄ averaging to -
7 27.9±1.4‰, C₂₆ to -29.3±1.0‰, and C₂₈ *n*-alkanoic acids to -31.0±0.9‰ (Figs. 2 and S3). For
8 the C₂₈ we find no significant downcore trend. C₂₄ shows the largest variations in $\delta^{13}\text{C}$ values
9 with generally more ¹³C-depleted values in the middle of the core (min: -30.7‰) compared to
10 the core-base and core-top (max: -24.3‰) (Fig. S3). For hydrogen isotopes, compounds are
11 also more D-depleted with increasing chain-length (C₂₄: -173±6‰; C₂₆: -182±7‰; C₂₈: -
12 185±6‰; Fig. 2). We observe downcore variations in δD values for C₂₆ and C₂₈ ranging from
13 -196 to -167‰.

14 Six water samples (two from inflows, two from Lake Karakuli and two from ponds nearby)
15 have been analysed for isotopic composition (Table 1). Both inflows show similar isotopic
16 signatures (ca. -83‰). The lake water averages +3.5‰ ($\delta^{18}\text{O}$) and +15‰ (δD) enriched
17 relative to the inflow due to evaporation. Closed ponds nearby are also evaporatively enriched
18 relative to inflow.

19

20 **5 Discussion**

21 **5.1 Origin of organic compounds and implications for source water**

22 **5.1.1 Molecular abundance distribution**

23 Organic compounds in lake sediments originate from a mixture of terrestrial and aquatic
24 organisms, with molecular abundance distributions and isotopic compositions that may be
25 diagnostic of source. Most plants contain a broad range of biomarkers (e.g. *n*-alkanes or
26 fatty acids) but the fingerprints of the different compound classes are mainly dominated by
27 compounds of a specific chain-length. Terrestrial and emergent aquatic plants for instance
28 produce higher proportional abundances of long-chain *n*- alkanes (e.g. C₂₉ and C₃₁) while
29 submerged macrophytes contain higher amounts of mid-chain *n*-alkanes (e.g. C₂₃ and C₂₅)
30 (Ficken et al., 2000; Aichner et al., 2010b). *n*-Alkanolic acids show a less distinct pattern
31 (Ficken et al., 2000), but also here long-chain compounds (e.g. C₂₈-FAs) are mostly

1 interpreted to be originated from terrestrial sources (e.g. Kusch et al., 2010; Feakins et al.,
2 2014).

3 In the sediments of Lake Karakuli the contribution of aquatic plants to the lipid pool is
4 considered to be relatively low compared to other Tibetan high altitude lakes. A submerged
5 aquatic plant sample collected close to the shore-line (ca. 20 cm water depth) shows a
6 dominance of C₁₆ and C₁₈-FAs and minor relative amounts of C₂₀ to C₃₀ even-chain FAs (see
7 Fig. S4). This fatty acid-pattern is in agreement with published fingerprints of other aquatic
8 plants collected on the Tibetan Plateau (Wang and Liu, 2012). Hence, the low relative
9 abundance of C₁₆ and C₁₈-FAs in our sediment samples suggests a relatively low contribution
10 of plant material derived from aquatic macrophytes to the sedimentary organic matter in Lake
11 Karakuli.

12 **5.1.2 Carbon isotopic signal**

13 Additional indication for the source of compounds comes from their carbon isotopic
14 signature. Lipids of terrestrial C₃-plants usually show values around -30 to -35‰, while
15 compounds derived from terrestrial C₄-plants and from submerged aquatic macrophytes can
16 reach significantly more enriched values in the range -15 to -20‰ (Chikaraishi and Naraoka
17 2005; Aichner et al, 2010a). The difference between C₃ and C₄-plants can be explained by
18 different isotopic fractionation in carbon assimilation of those two plant types, while the
19 enriched values of submerged aquatic plants are due to the uptake of different carbon sources
20 i.e. isotopically enriched bicarbonate instead of dissolved CO₂ (Allen and Spence, 1981; Prins
21 and Elzenga, 1989).

22 In our sediment core from Lake Karakuli δ¹³C-values of the C₂₈-FA are similar to that of
23 terrestrial C₃-plants without a clear trend (Fig. 2; Fig. S3). Thus, we conclude that this
24 compound is predominantly derived from terrestrial C₃ grasses in the lake catchment. δ¹³C
25 values of C₂₄ and C₂₆-*n*-alkanoic acids are slightly higher than for C₂₈, indicating an
26 increasing contribution of submerged aquatic plant material and/or lipids derived from C₄-
27 plants with decreasing chain lengths.

28 δ¹³C values of C₂₄ *n*-alkanoic acids are controlled by relative contributions of aquatic
29 macrophytes and/or macrophyte productivity, with higher productivity leading to higher δ¹³C
30 values (Aichner et al., 2010b). We hypothesize that a higher proportional input of aquatic
31 material to the sedimentary organic matter is indicative of warmer and possibly also drier
32 conditions. Longer ice-free periods and a lower lake level could be the driving factors behind
33 enhanced macrophyte growth during warmer years.

1 C₄-plants are widely absent on the central and eastern Tibetan Plateau at present, but they are
2 wide-spread in Central Asian deserts and some *Chenopodiaceae* which use the C₄-pathway
3 have occasionally been observed at high altitude alpine deserts of the Pamir (Sage et al.,
4 2011). Thus we cannot totally exclude the contribution of C₄-derived lipids to the sedimentary
5 organic matter of Lake Karakuli, however, we consider these sources as of secondary
6 importance. Nevertheless, if we have underestimated the input of alkanolic acids derived from
7 C₄-plants this would not bias the overall interpretation, because higher abundances of C₄-
8 plants resulting in higher sedimentary $\delta^{13}\text{C}$ would indicate a drier/warmer climate, which is
9 similar to the hypothesis that drying/warming leads to increased macrophyte productivity.

10 **5.1.3 Hydrogen isotopic signal**

11 Hydrogen isotopes provide further evidence for the origins of C₂₄ and C₂₆ or C₂₈ *n*-alkanoic
12 acids. The average δD values of C₂₄ are ca. 9-12‰ higher than that of C₂₆ and C₂₈ (Fig. 2). A
13 different water source i.e. isotopically enriched lake water (see Tab. 1) instead of water
14 derived from precipitation or snow-melt could explain this. We assume that C₂₄ is derived
15 from mixed aquatic and terrestrial sources, while C₂₈ and also C₂₆ can be considered as of
16 mainly terrestrial origin.

17 The δD -values of these terrestrial biomarkers is representative of the hydrogen isotopic
18 composition of the source water which –for terrestrial plants– could be expected to be spring
19 and summer precipitation during the growing season (Sachse et al., 2012), although a
20 contribution of D-depleted melt-water from snow in the early spring growth period is highly
21 likely (Fan et al., 2013). The fractionation factors between source water and lipids are variable
22 but previous studies found that for terrestrial C₃-grasses they average to $-149\pm 28\text{‰}$ (n=47) for
23 the C₂₉ *n*-alkane, while they are ca. $-134\pm 28\text{‰}$ (n=53) for C₄-grasses and in similar range for
24 forbs (Sachse et al., 2012). In arid ecosystems, soil-water evaporation (for grasses; Smith and
25 Freeman, 2006) and transpiration from the leaf, lead to isotopic enrichment of leaf water
26 above the meteoric water (Feakins and Sessions, 2010; Kahmen et al., 2013a and b). Recent
27 results from the central Tibetan Plateau, a similar environmental setting to our study,
28 quantified the apparent isotopic fraction between meteoric water and *n*-alkanes to be ca. -95‰
29 due to ca. $+70\text{‰}$ evapotranspirational isotopic enrichment above meteoric water (Günther et
30 al., 2013). This is in agreement with the average fractionation from Feakins and Sessions
31 (2010) who suggested ca. -95‰ as net fractionation factor between meteoric water and leaf
32 wax *n*-alkanes in an arid ecosystem (southern California), and found similar values for *n*-
33 alkanolic acids in a later study from that region (Feakins et al., 2014).

1 While the fractionation was not directly determined on modern plant *n*-alkanoic acids in this
2 catchment, based on core-top δD_{lipid} -values of ca. -190‰ and knowledge of hydrogen isotope
3 values of modern precipitation and waters in the catchment we can infer a reasonable
4 catchment average apparent fractionation (Fig. 3). Summer precipitation in the catchment
5 averages ca. -45‰ at Lake Karakuli, compared to mean annual precipitation average of ca. -
6 90‰ (derived from the Online Isotopes in Precipitation Calculator, OIPC; Bowen and
7 Revenaugh, 2003.; Fig. 4b). If the summer precipitation (-45‰; OIPC) is indicative of source
8 water, and given the measured sedimentary value of C_{28} *n*-alkanoic acids (-190‰) we would
9 compute an apparent fractionation of ca. -150‰ (see supplement S5 for formula to calculate
10 isotopic fractionation factors). Whereas if we use mean annual precipitation (ca. -90‰; OIPC)
11 then the calculated apparent fractionation would be ca. -110‰ which is closer to the reported
12 fractionation factors for arid ecosystems (Feakins and Sessions, 2010; Günther et al., 2013).

13 The δD -values of the two lake inflows sampled in September 2008 (average -83‰; Table 1)
14 provide a reasonable constraint on catchment average water isotopic composition in
15 September, presumably including a mix of contributions from precipitation runoff,
16 groundwater, and snow melt from winter precipitation and higher elevations. A calculated
17 source water δD value based on published fractionation factors mentioned above (ca. -95‰)
18 would be -110‰ (Fig. 3) which is in range of late-winter/early spring precipitation in the
19 study area according to OIPC-data (Fig. 4b). These are helpful constraints on the proxy,
20 however, regardless of knowing the exact season of source water and the appropriate
21 fractionation which are needed for absolute isotopic conversions, we can infer relative
22 variations in δD values of the C_{28} *n*-alkanoic acid down core in terms of variations in the δD
23 of precipitation. We therefore use the δD values of the C_{28} and C_{26} *n*-alkanoic acids to
24 reconstruct past variations in the isotopic composition of precipitation.

25 **5.2 Controls on the isotopic signature of precipitation in the eastern Pamir**

26 **5.2.1 Monthly signal**

27 The isotopic composition of precipitation is influenced by multiple isotope effects including
28 those associated with precipitation amount, condensation temperature, or vapour source (Gat,
29 1996). In subtropical and tropical latitudes, the ‘amount effect’ has usually been identified as
30 most relevant controlling factor with lower δD values reflecting more humid episodes in
31 sedimentary records (Schefuss et al., 2005; Tierney et al., 2008, Lee et al., 2008). At mid- and
32 high latitudes temperature and vapour source mostly have interpreted to be the dominant

1 factors (Dansgaard, 1964; Thompson, 2000; Rach et al., 2014). In addition, large scale
2 circulation changes or a shift in the balance of two or more different moisture sources and
3 transport trajectories can result in isotopic shifts over time (Dansgaard, 1964; Thompson,
4 2000; Rach et al., 2014).

5 Evaluating isotopes of precipitation in context with climatic parameters in Asia, Araguas-
6 Araguas et al. (1998) and Yao et al. (2013) came to the conclusion that the amount effect is
7 the dominant factor in monsoonal east Asia while in arid Central Asia temperature mainly
8 controls δD and $\delta^{18}O$ values of precipitation. The closest meteorological stations to Lake
9 Karakuli are the station at Bulun Kul (ca. 30 km northeast) and Taxkorgan (ca. 80 km south).
10 Both stations record low winter precipitation and slightly enhanced amounts during the
11 summer (Fig., 4a and b). Higher isotopic values in the summer compared to the winter (Yao et
12 al., 2013; Bowen and Revenaugh, 2003) suggest that monthly values are indeed driven by
13 temperature. If these seasonal controls are also determining interannual variations in the
14 isotopic composition of precipitation then temperature is likely to be a major factor explaining
15 the reconstructed hydrogen isotopic variability.

16 We also observe amount effect modulation of the summer season precipitation isotopes
17 associated with increased precipitation totals in June 2004 and more pronounced in June
18 2005 (Fig. 4a), which lowers the $\delta^{18}O$ values. This amount effect lowers the summer
19 precipitation isotopic composition, dampens the seasonality of mean precipitation of isotopic
20 values, and lowers the integrated annual precipitation isotopic composition. Hence in drier
21 years average δD values will be D-enriched relative to wetter years; and likewise warmer
22 years will be D-enriched relative to colder years (Fig. 4b). Given the low precipitation
23 amounts in this arid region today, the amount effect is likely to remain secondary to the
24 temperature controls on isotopic composition apparent in the seasonal cycle.

25 **5.2.2 Annual/seasonal signal**

26 To further establish the connections between climate anomalies and isotopic signatures of
27 precipitation in Central Asia, we compare instrumental data and climate model simulations.
28 At Taxkorgan meteorological station we find a negative correlation between annual
29 temperature and precipitation amount over a period of 43 yrs (1957-2000; Fig. 5; data
30 provided from Tian et al., 2006). Similar trends can be observed when comparing simulated
31 data over a period of 50 yrs (1958-2009; Fig. 5). We use the LMDZ4 climate model (Hourdin
32 et al., 2006) to characterize the climatic processes in our study area (as described in Lee et al.
33 2012). We find higher annual precipitation amounts in the LMDZ4 model simulations

1 compared to instrumental observations at Taxkorgan meteorological stations. This is related
2 to the scale of the model resolution of $3.75^\circ \times 2.5^\circ$ (Lee et al., 2012) which includes the
3 relatively high precipitation amounts in higher altitudes during winter (Seong et al., 2009a and
4 b; Wu et al., 2008) within the grid box. Significant negative correlations ($r=0.58$; $p<0.0001$)
5 between temperature and precipitation amount can be inferred for the summer months (April-
6 September), while comparisons over the winter or whole year deliver non-significant
7 correlations ($p>0.01$; Fig. 5).

8 As a consequence of the negative correlation between temperature and precipitation amount
9 we observe positive/negative correlations between precipitation isotopes and those climatic
10 parameters for our larger study area (Fig. 6). Considering temperature, we found a positive
11 correlation ($0.4 < r < 0.6$) for both winter and summer over large parts of Central Asia
12 indicating the broad regional significance of our record. For the summer, no correlations are
13 seen in India and SE Asia, where distinct monsoonal circulation and precipitation patterns
14 exert independent controls on the isotopic values of precipitation (Morill et al., 2003; Yao et
15 al., 2013). Considering precipitation amount, negative correlations ($-0.6 < r < -0.2$) can be
16 deduced for the summer months for a large region around Lake Karakuli, spanning from SW
17 to NE and covering parts of Iran, Central Asia and NW China. During winter, no correlation
18 can be observed directly at the location of the lake, however, precipitation isotopes seem to
19 negatively correlate with precipitation amounts located westwards to our study area (Fig. 6).

20 In a recent study Tian et al. (2006) found a positive correlation between $\delta^{18}\text{O}$ in the local
21 Muztagh Ata ice core (which covers the period 1957-2003) and annual temperatures from
22 Taxkorgan climate station. In contrast they found no significant relationship between ice-core
23 $\delta^{18}\text{O}$ and annual precipitation amount at Taxkorgan (Tian et al., 2006). Different precipitation
24 dynamics between middle and high altitudes, and/or seasonal differences, as supported by our
25 LMDZ4-data, could explain this discrepancy. Elevation differences may play a role in
26 different precipitation patterns and these may be associated with isotope effects. The Muztagh
27 Ata glacier accumulation zone receives higher annual precipitation amounts and also a higher
28 proportional input from winter precipitation compared to lower altitudes (Seong et al., 2009a
29 and b). Whilst instrumental and modelling data inferred a slight increase of precipitation
30 amount throughout the last 50 years in the westernmost part of China (Yao et al., 2012; Zhang
31 and Cong, 2014), a decreasing accumulation rate at the Muztagh Ata ice core since 1976 was
32 measured by Duan et al. (2007). Even if the instrumental data from Taxkorgan do not show a
33 significant trend in precipitation amount between 1957 and 2000, this does not rule out

1 changes of snowfall at higher altitudes. Increasing temperatures could have further
2 contributed to the lower observed accumulation rates.

3 Since temperature and precipitation amounts are anti-correlated on an interannual timescale
4 (Fig. 5), we interpret low δD values to indicate both relatively cool and wet conditions. In
5 addition to fluctuations in mean annual precipitation isotopes, snow-melt and delivery to
6 plants may vary. We suggest that a high proportional contribution of water derived from
7 snow-melt, after relatively long and wet winters with high amounts of snowfall, can further
8 lead to more negative δD leaf wax values.

9 **5.3 Paleoclimatic interpretation of downcore data**

10 δD and $\delta^{13}C$ values from Lake Karakuli sediment core suggest relatively warm and dry
11 conditions between ca. 4-3.5 kyrs BP (Fig. 7). $\delta^{13}C$ values are highest for C_{24} during this
12 interval and even C_{28} shows slightly enriched values ($>-30\text{‰}$; Fig. S3). Also δD shows
13 maximum values during this episode. Even though an increased input from C_4 -plants or
14 enhanced productivity of aquatic macrophytes could slightly have biased δD -values towards a
15 more positive signal, we infer that this period probably was the warmest/driest in our studied
16 time-interval. After 3.5 kyrs a gradual cooling trend started (interrupted by a warmer/drier
17 period between ca. 3.0 and 2.7 kyrs BP), peaking in coolest and wettest conditions around 2.5
18 kyrs BP. Between ca. 2.5 and 1.9 kyrs BP we observe a reversal to a slightly warmer and drier
19 climate, based on δD evidence. We note that the $\delta^{13}C$ values are rather variable and
20 inconclusive in this core-section, and we observe an offset between $\delta D-C_{26}$ and $\delta D-C_{28}$ (these
21 are normally within analytical error of each other). We hypothesize that a warming influenced
22 precipitation isotopes but that the change wasn't intense and stable enough to trigger a large-
23 scale ecosystem response to be recorded in the $\delta^{13}C$ values. Between ca. 1.9 and 1.4 kyrs BP,
24 cool and wet conditions occurred again before returning to a warm and dry episode from ca.
25 1.4 to 0.6 kyrs BP (possibly interrupted by a cooling event around 1 kyrs BP). The last 0.6
26 kyrs have been mainly cool and wet again, except for the last ca. 100 years, where the
27 topmost three samples of the sediment core indicate another reversal to relatively warm and
28 dry conditions.

29 Enhanced precipitation, rather than lower temperatures, has been argued to be the main
30 driving force behind growth of glaciers in Asian high-altitude regions (Seong et al., 2009b).
31 The cool/wet episodes deduced from our organic geochemical record match relatively well to
32 reconstructed glacial advances at Mts. Muztagh Ata and Kongur Shan. On basis of ^{10}Be -

1 dating of erratic boulders Seong et al. (2009a) estimated maximal glacial advances at 4.2 ± 0.3
2 kyrs, 3.3 ± 0.6 kyrs, 1.4 ± 0.1 kyrs, and a few hundred years before present (Fig. 7). Further, the
3 δD -data are in good agreement with silt-contents in the same sediment core (Fig. 7). These
4 have been interpreted to be influenced by glacial input and thus higher contents indicating
5 cooler/wetter conditions (Liu et al., 2014).

6 Our interpretation of lower δD -values indicating both relatively cool and wet conditions fits
7 well with results from other late Holocene records in arid Central Asia (Fig. 8c, e and g). The
8 Little Ice Age (LIA) corresponds to the cool/humid period between 0.6 and 0.1 cal. ka BP at
9 Lake Karakuli and has been well documented as a widely humid episode in arid Central Asia
10 (paleoclimatic data compiled in Chen et al., 2010; Fig. 8c). For instance, the Guliya ice core,
11 located ca. 630 km SE from Lake Karakuli, shows relatively high accumulation rates during
12 that period (Fig. 8e), indicating that higher precipitation amounts and not just higher effective
13 moisture (induced by decreased evaporation during cooler conditions) was the main driving
14 force behind e.g. higher lake levels. This very much contrasts the situation in
15 eastern/monsoonal Asia where many records show a relatively dry LIA due to a weakened
16 summer monsoon (Chen et al., 2010 and references therein).

17 Similarly a number of records have shown a pronounced warm/dry period during the
18 Medieval Climate Anomaly (MCA; Fig 8 c,e; Chen et al., 2010; Lauterbach et al., 2014;
19 Esper et al., 2002) also seen in our record from Late Karakuli. At ca. 1 cal. ka BP we observe
20 a ca. 100-year interruption of this event indicated by three samples with lower δD -values.
21 Recently, Lei et al. (2014) observed a similar spike in carbonate $\delta^{18}O$ values from Lake Sasi
22 Kul, which is located ca. 190 km west of our study site (Fig. 8b). Thus we hypothesize that
23 this interruption was not just a local phenomenon. Warm and dry conditions during the MCA
24 have also been observed at Kashgar (western Tarim Basin; just ca. 150 km north of Lake
25 Karakuli; Zhao et al., 2012), and from from Lakes Bangong Co on the western Tibetan
26 Plateau (Gasse et al., 1996) and large Karakul in the Tajik Pamir (Mischke et al., 2010).

27 Applying these findings to the complete record we see fluctuating climatic conditions
28 throughout the late Holocene with clearly identifiable warmer/drier and cooler/wetter
29 episodes (Fig. 8). During the oldest section of our record (ca. 4.2-3.4 kyrs BP) average
30 conditions appeared having been warmer and drier than during the medieval and today,
31 followed by a general (even though non-continuous) cooling trend until ca. 2.4 kyrs BP. A
32 cool and wet phase of roughly 1000 years starting at ca. 3.5 kyrs BP has been observed in
33 numerous global climate records (Mayewski et al., 2004). At the nearby oasis of Kashgar,

1 conditions prevailed relatively wet from ca. 4.0 until ca. 2.6 kyrs BP (Zhao et al., 2012). At
2 the large Lake Karakul in Tajikistan a rapid drop of TOC-contents occurred at ca. 3.5 cal. ka
3 BP, indicating a drop of lake productivity probably induced by low-temperatures and
4 eventually associated with shorter ice-free periods in the summer (Mischke et al., 2010; Fig.
5 8h). At Lake Balikun (northeastern Xinjiang) a reversal to wetter conditions occurred after a
6 pronounced dry event lasting from 4.3-3.8 kyrs BP (An et al., 2012). In Lake Manas (northern
7 Xinjiang) a wet episode was reconstructed for 4.5-2.5 kyrs BP, interrupted by a short dry
8 period between 3.8-3.5 kyrs BP (Rhodes et al., 1996). Low $\delta^{18}\text{O}$ -values in the Guliya ice core
9 between 3.5 and 3.0 kyrs BP also give evidence for low temperatures on the northwestern
10 Tibetan Plateau (Thompson et al., 1997) while in the southern Tarim Basin a rapid shift to
11 wetter conditions at ca. 3.0 kyrs BP have been observed (Zhong et al., 2007).

12 After a ca. 500 year slight warming (ca. 2.4-1.9 kyrs BP; synchronous with the Roman Warm
13 Period; RWP), another reversal into cool and wet condition occurred, peaking at ca. 1.8-1.6
14 kyrs BP (often referred to as Dark Ages Cool Period, DACP, or Migration Period). Both of
15 these events have also been observed in the nearby Kashgar (Zhao et al., 2012). Afterwards
16 that the climatic trend gradually transitioned into the above mentioned warm period during the
17 medieval, followed by the LIA and the current warming period (CWP), the latter indicated by
18 increased δD values in the topmost three samples of the sediment core.

19 **5.4 Implications for Central Asian climate dynamics**

20 The sequence of relatively cool/wet and warm/dry episodes displays coherency with other
21 records of Northern Hemisphere climate records. There is a similarity between cyclicality of
22 cooling events at Lake Karakuli, Northern Atlantic ice-rafting events (Fig 8j; Bond et al.,
23 2001) and strengthening phases of the Siberian High (the anticyclonic high pressure ridge
24 over Siberia), the latter recorded by $[\text{K}^+]$ increases in the GISP2 ice core between ca. 3.5-2.8
25 and 0.5-0.2 kyrs BP (Fig 8i; Mayewski et al., 1997). Further, throughout the last ca. 1000
26 years, δD values of leaf waxes in Lake Karakuli are correlated with the mode of the North
27 Atlantic Oscillation (NAO), showing more positive values during the current and medieval
28 positive mode and more negative values during the LIA-negative mode (Fig. 8f; Trouet et al.,
29 2009).

30 The interplay between the dominant atmospheric circulation systems in Central Asia – the
31 Siberian High, the mid-latitude Westerlies and partly the Indian Summer Monsoon– as well as
32 orographic influences, lead to complex climatic patterns. Trajectory studies in the modern

1 atmosphere, as well as inventories of dust particles in ice cores, suggest the mid-latitude
2 Westerlies as primary source of moisture during winter and spring, with the North Atlantic,
3 the Mediterranean, the Black and Caspian Sea as possible regions of origin (Lei et al., 2014;
4 Seong et al., 2009a and b; Wu et al., 2008). The Siberian High delivers cool but also relatively
5 dry air during winter. The absence of sea-salt i.e. in the Muztagh Ata ice core (Aizen et al.,
6 2001; Seong et al., 2009b) further gives evidence for a minor importance of the Indian
7 Monsoon, and for mid-latitude Westerlies and local convection to be the most important
8 moisture sources during the summer.

9 Even though Lake Karakuli receives some moisture in spring (Fig. 4), regions which are
10 located as close as 190 km westwards at a similar altitude, such as Lake Sasi Kul and other
11 parts of the central and western Pamirs receive much higher proportions and amounts of
12 winter and spring precipitation (Lei et al., 2014; Mische et al., 2001). Variations of strength
13 and tracks of the Westerlies and related movement of the Polar Front (Machalett et al., 2008)
14 could have influenced the amount of winter and spring moisture which has reached the
15 Karakuli-region in the past. Lei et al. (2014) suggested that during negative NAO-modes (e.g.
16 during the LIA) the storm tracks were moving further southwards, leading to wetter
17 conditions in the Mediterranean and higher amounts of moisture been transported into Central
18 Asian realms of the same latitude. In contrast other authors proposed a more complex
19 interplay between the Eurasian and Pacific circulation systems on basis of modelling data, and
20 a generally higher delivery of moisture into Central Asia during episodes of strengthened
21 Westerlies (i.e. positive NAO-modes) (Syed et al., 2010; Syed, 2011). Recently, a possible
22 negative correlation between lower winter precipitation in the Mediterranean (positive NAO-
23 mode) and higher winter precipitation at Son Kol (central Tien Shan; ca. 400 km north of
24 Lake Karakuli) was also suggested by Lauterbach et al. (2014) on basis of $\delta^{15}\text{N}$ -data on total
25 nitrogen (Fig. 8d).

26 Based on our data, we hypothesize that the relatively wet episodes recorded in our sediment
27 core from Lake Karakuli were mainly caused by increased late-winter and spring precipitation
28 derived from mid-latitude Westerlies. Cooling/wetening periods at 3.5 cal. ka BP and
29 between 1.9 and 1.5 kyrs BP (DACP) are simultaneous with increased winter precipitation at
30 Son Kol (Fig. 8d), indicating common climatic variations in the eastern Pamirs and the central
31 Tien Shan. For the LIA, this connection is less pronounced. Instead, for the last ca. 1.5 kyrs
32 BP, we see a close similarity to isotopic trends in the central Pamirs (Fig. 8b), which in turn
33 drift apart between 1.5 and 2.5 kyrs BP. An explanation for this could be the increased

1 influence of the significantly strengthened Siberian High during the LIA (Fig. 8i). This
2 possibly weakened the mid-latitude Westerlies or pushed their tracks further to the south,
3 resulting in comparably drier conditions at more northern regions such as the Tien Shan, but
4 wetter conditions in the central and eastern Pamirs (Lei et al., 2014). A similar mechanism
5 could explain the climatic pattern in the eastern Pamirs at present, with low winter and spring
6 precipitation at low altitudes during the current positive NAO-mode and Westerlies
7 penetrating more to the North, while the central Pamirs still receive high winter precipitation.

8 Despite a slight increase in total precipitation amount over the last 50 years in the dry areas of
9 Western China (Yao et al., 2012; Zhang and Cong, 2014), effective moisture in our study area
10 has decreased due to rising temperatures. The two closed ponds and Lake Karakuli itself show
11 clear geomorphological evidence for recent shrinking (field observations) and isotopic
12 evidence for evaporative enrichment above meteoric waters (Table 1). This is in contrast to
13 several endorheic lakes in Central Asia, whose lake levels are rising due to the currently
14 increased meltwater input from receding glaciers (e.g. Bosten Lake; Wünnemann et al., 2006;
15 or large Lake Karakul in Tajikistan, Mischke et al., 2010).

17 **6 Conclusion**

18 The biomarker isotopic record from Lake Karakuli, eastern Pamirs, shows distinct episodes of
19 relatively cool/wet and warm/dry climate over the last 4200 years. Variations in the North
20 Atlantic conditions and Siberian High both appear to show similarities with variations
21 captured in our biomarker isotopic record, including notable excursions associated around 3.5
22 kyrs, the MCA, and the LIA. However, there are also indications for complex responses of
23 regional climate, i.e. different responses between the western (e.g. western and central Pamir),
24 eastern (e.g. eastern Pamir) and northern (e.g. Tien Shan) parts of Central Asia. These
25 regional differences are thought to arise from changes in the dynamics and interplay of the
26 involved large scale atmospheric circulation systems, especially the strengths and pathways of
27 the Westerlies. Our data provide evidence that the transition between regions of summer-only
28 and winter/spring dominated precipitation could have been a key factor for local climate in
29 the past. They further show a rapid aridification in the eastern Pamir during the last 50-100
30 years.

32 **Acknowledgements**

1 This work was supported by the German Academic Exchange Service (DAAD) postdoctoral
2 fellowship to B. Aichner at the University of Southern California (USC) and by USC and the
3 U.S. National Science Foundation (Grant No. 1002656) to S. Feakins for analytical costs.
4 Funding from the Deutsche Forschungsgemeinschaft (DFG), the China Global Change
5 Research Program (Grant No. 2012CB956101), and the National Science Foundation China
6 (Grant No. 41072131) supported the fieldwork, the sample transport, and the radiocarbon
7 dating. We thank Hanno Meyer and Lutz Schoenicke (AWI Potsdam) for providing isotopic
8 data of water samples. We are further grateful for help during field work (Jian Ni and Yang
9 Bo), for assistance with core sampling (Yongbo Wang) and for analytical support at USC
10 (Miguel Rincon).

11

12 **References**

13 Aichner, B., Herzsuh, U., and Wilkes, H.: Influence of aquatic macrophytes on stable
14 carbon isotope signatures of sedimentary organic matter in lakes on the Tibetan Plateau, *Org.*
15 *Geochem.*, 41 (7), 706-718, 2010a.

16 Aichner, B., Herzsuh, U., Wilkes, H., Mischke, S., and Zhang, C.: Biomarker and
17 compound-specific carbon isotope evidence for changing environmental and carbon-limiting
18 conditions at Koucha Lake, eastern Tibetan Plateau, *J. Paleolimn.*, 43 (4), 873-899, 2010b.

19 Aichner, B., Herzsuh, U., Wilkes, H., Vieth, A., and Böhner, J.: δD values of *n*-alkanes in
20 Tibetan lake sediments and aquatic macrophytes a surface sediment study and application to a
21 16 ka record from Lake Koucha, *Org. Geochem.*, 41 (8), 779-790, 2010c.

22 Aizen, E.M., Aizen, V.B., Melack, J.M., Nakamura, T., and Ohta, T.: Precipitation and
23 atmospheric circulation patterns at mid-latitudes of Asia, *Int. J. Climatol.*, 21, 535-556, 2001.

24 Allen, E.D., and Spence, D.H.N.: The differential ability of aquatic plants to utilize the
25 inorganic carbon supply in fresh water, *New Phytol.*, 87(2), 269-283, 1981.

26 An, C.B., Feng, Z.D., and Barton, L.: Dry or humid? Mid-Holocene humidity changes in arid
27 and semi-arid China, *Quaternary Sci. Rev.*, 25, 351-361, 2006.

28 An, C.B., Lu, Y., Zhao, J., Tao, S., Dong, W., Li, H., Jin, M., and Wang, Z.: A high-
29 resolution record of Holocene environmental and climatic changes from Lake Balikun
30 (Xinjiang, China): Implications for central Asia, *Holocene*, 22(1), 43-52, 2012.

1 Araguás-Araguás, L., Froehlich, K., and Rozanski, K.: Stable isotope composition of
2 precipitation over southeast Asia, *J. Geophys. Res.-Atmos.*, 103 (D22), 28721-28742, 1998.

3 Blaauw, M., and J. A. Christen.: Flexible paleoclimate age-depth models using an
4 autoregressive gamma process, *Bayesian Anal.*, 6(3), 457-474, 2011.

5 Bond, G., Kromer, B., Beer, J., Muscheler, R., Evans, M., Showers, W., Hoffmann, S., Lotti-
6 Bond, R., Hajdas, I., and Bonani, G.: Persistent solar influence on North Atlantic climate
7 during the Holocene, *Science*, 294, 2130-2136, 2001.

8 Bowen G. J., and Revenaugh J.: Interpolating the isotopic composition of modern meteoric
9 precipitation, *Water Resour. Res.*, 39(10), 1299-1311, 2003.

10 Boomer, I., Wünnemann, B., Mackay, A.W., Austin, P., Sorrell, P., Reinhardt, C., Keyser, C.,
11 Guichard, F., and Fontugne. M.: Advances in understanding the late Holocene history of the
12 Aral Sea region, *Quatern. Int.*, 194, 79-90, 2009.

13 Chen, F.H., Yu, Z.C., Yang, M.L., Ito, E., Wang, S., Madsen, D.B., Huang, X., Zhao, Y.,
14 Sato, T., Birks, J.B., Boomer, I., Chen, J., An, C., and Wünnemann, B.: Holocene moisture
15 evolution in arid central Asia and its out-of-phase relationship with Asian monsoon history,
16 *Quaternary Sci. Rev.*, 27, 351-364, 2008.

17 Chen, F.H., Chen J.H., Holmes, J.A., Boomer, I., Austin, P., Gates, J.B., Wang, N.L., Brooks,
18 S.J., and Zhang, J.W.: Moisture changes over the last millennium in the arid central Asia: A
19 review, synthesis and comparison with monsoon region, *Quaternary Sci. Rev.*, 29 (7-8), 1055-
20 1068, 2010.

21 Cheng. H., Zhang, P.Z., Spötl, C., Edwards, R.L., Cai, Y.J., Zhang, D.Z., Sang, W.C., Tan,
22 M., and An, Z.S.: The climatic cyclicity in semiarid-arid central Asia over the past 500,000
23 years. *Geophys. Res. Lett.*, 39, L01705, doi:10.1029/2011GL050202, 2012

24 Chikaraishi, Y., and Naraoka, H.: $\delta^{13}\text{C}$ and δD identification of sources of lipid biomarkers in
25 sediments of Lake Haruna (Japan), *Geochim. Cosmochim. Ac.*, 69 (13), 3285-3297, 2005

26 Dansgaard, W.: Stable isotopes in precipitation. *Tellus* 16 (4), 436-468. 1964.

27 Duan, K., Yao, T., Wang, N.L., Tian, L.D., Xu, B.Q., and Wu, G.J.: Records of precipitation
28 in the Muztag Ata ice core and its climate significance to glacier water resources. *J. Glaciol.*
29 *Geocryol.*, 29 (5), 680-684, 2007.

30 Esper, J., Schweingruber, F.H., Winiger, M.: 1300 years of climatic history for Western
31 Central Asia inferred from tree-rings, *Holocene*, 12 (3), 267-277, 2002.

1 Fan, L.L., Tang., L.S., Wu, L.F., Ma., J., and Li, Y.: The limited role of snow water in the
2 growth and development of ephemeral plants in a cold desert. *J. Veg. Sci.*, 25, 681-690, 2014.

3 Feakins, S.J., Sessions, A.L., Controls on the D/H ratios of plant leaf waxes from an arid
4 ecosystem. *Geochim. Cosmochim. Ac.*,74, 2128-2141, 2010.

5 Feakins, S.J., Kirby, M.E., Cheetham, M.I., Ibarra, Y., and Zimmerman, S.R.H.: Fluctuation
6 in leaf wax D/H ratio from a southern California lake records significant variability in
7 isotopes in precipitation during the late Holocene, *Org. Geochem.*, 66, 48-59, 2014.

8 Ficken, K.J., Li, B., Swain, D.L., and Eglinton, G.: An *n*-alkane proxy for the sedimentary
9 input of submerged/floating freshwater aquatic macrophytes. *Org. Geochem.*, 31, 745-749,
10 2000.

11 Gasse, F., Fontes, J.C., VanCampo, E., and Wei, K.: Holocene environmental changes in
12 Bangong Co basin (western Tibet). 4. Discussion and conclusions. *Palaeogeog. Palaeoclim.*
13 *Palaeoecol.*, 120, 79-92,1996.

14 Gat, J.R.: Oxygen and hydrogen isotopes in the hydrologic cycle. *Annu. Rev. Earth Pl. Sci.*,
15 24, 225-262, 1996.

16 Günther, F., Aichner, B., Siegwolf, R., Xu, B.Q., Yao, T., and Gleixner, G.: A synthesis of
17 hydrogen isotope variability and its hydrological significance at the Qinghai-Tibetan Plateau,
18 *Quatern. Int.*, 313-314, 3-16, 2013.

19 Herzsuh, U.: Paleo-moisture evolution in monsoonal Central Asia during the last 50,000
20 years, *Quaternary Sci. Rev.*, 25, 163-178, 2006.

21 Hourdin, F., Musat, I., Bony, S., Braconnot, P., Codron. F., Dufresne, J.L., Fairhead, L.,
22 Filiberti, M.A., Friedlingstein, P., Grandpeix, J.Y., Krinner, G., LeVan, P., Li, Z.X., and Lott,
23 F.: The LMDZ4 general circulation model: Climate performance and sensitivity to
24 parametrized physics with emphasis on tropical convection, *Clim. Dyn.*, 27, 787-813, 2006.

25 Huang , X., Oberhänsli, H., von Suchodoletz, H., and Sorrell, P.: Dust deposition in the Aral
26 Sea: Implications for changes in atmospheric circulation in central Asia during the past 2000
27 years. *Quaternary Sci. Rev.*, 30, 3661-3674, 2011.

28 Kahmen, A., Hoffmann, B., Schefuß, E., Arndt, S.K., Cernusak, L.A., West, J.B., and Sachse,
29 D.: Leaf water deuterium enrichment shapes leaf wax *n*-alkane δD values of angiosperm
30 plants II: observational evidence and global implications, *Geochim. Cosmochim. Ac.*, 111,
31 50-63, 2013a.

1 Kahmen, A., Schefuss, E., and Sachse, D.: Leaf water deuterium enrichment shapes leaf wax
2 *n*-alkane δ D values of angiosperm plants I: experimental evidence and mechanistic insights,
3 *Geochim. Cosmochim. Ac.*, 111, 39-49, 2013b.

4 Kusch, S., Rethemeyer, J., Schefuß, E., and Mollenhauer, G.: Controls on the age of vascular
5 plant biomarkers in Black Sea sediments, *Geochim. Cosmochim. Ac.*, 74, 7031-7047, 2010.

6 Lauterbach, S., Witt, R., Plessen, B., Dulski, P., Prasad, S., Mingram, J., Gleixner, G.,
7 Hettler-Riedel, S., Stebich, M., Schnetger, B., Schwalb, A., and Schwarz, A.: Climatic
8 imprint of the mid-latitude Westerlies in the Central Tian Shan of Kyrgyzstan and
9 teleconnections to North Atlantic climate variability during the last 6000 years, *The*
10 *Holocene*, 24, 970-998, 2014.

11 Lee, J.-E., and Fung, I.: “Amount effect” of water isotopes and quantitative analysis of post-
12 condensation processes, *Hydrol. Processes*, 22, 1-8, 2008.

13 Lee, J.E., Risi, C., Fung, I., Worden, J., Scheepmaker, R.A., Lintner, B., and Frankenberg, C.:
14 Asian monsoon hydrometeorology from TES and SCIAMACHY water vapor isotope
15 measurements and LMDZ simulations: Implications for speleothem climate record
16 interpretation, *J. Geophys. Res.*, 117, D15112, doi:10.1029/2011JD017133, 2012.

17 Lei, Y., Tian, L.D., Bird, B.W., Hou, J., Ding, L., Oimahmadov, I., and Gadoev, M.: A 2540-
18 year record of moisture variations derived from lacustrine sediment (Sasikul Lake) on the
19 Pamir Plateau, *The Holocene*, 24, 761-777, 2014.

20 Liu, X., Herzsuh, U., Shen, J., Jiang, Q., and Xiao, X.: Holocene environmental and
21 climatic changes inferred from Wulungu Lake in northern Xinjiang, China. *Quaternary*
22 *Res.*, 70, 412-425, 2008.

23 Liu, X., Herzsuh, U., Wang, Y., Kuhn, G., Yu, Z.: Glacier fluctuations of Muztagh Ata and
24 temperature changes during the late Holocene in westernmost Tibetan Plateau, based on
25 glaciolacustrine sediment records, *Geophys. Res. Lett.*, 41, 6265-6273, 2014.

26 Liu, Z.H., Henderson, A.C.G. and Huang, Y.S.: Regional moisture source changes inferred
27 from Late Holocene stable isotope records, *Adv. Atmos. Sci.*, 25, 1021-1028, 2008.

28 Machalett, B., Oches, E.A., Frechen, M., Zöller, L., Hambach, U., Mavlyanova, N.G.,
29 Marković, S.B., and Endlicher, W.: Aeolian dust dynamics in central Asia during the
30 Pleistocene: Driven by the long-term migration, seasonality, and permanency of the Asiatic
31 polar front, *Geochem. Geophys. Geosyst.* 9, Q08Q09, doi:10.1029/2007GC001938, 2008.

1 Mayewski, P. A., Meeker, L.D., Twickler, M.S., Whitlow S., Yang, Q., Lyons, W.B., and
2 Prentice, M.: Major features and forcing of high-latitude northern hemisphere atmospheric
3 circulation using a 110,000-year-long glaciochemical series, *J. Geophys. Res.*, 102(C12),
4 26345-26366, 1997.

5 Mayewski, P.A., Rohling, E.E., Stager, J.C., Karlén, W., Maasch, K.A., Meeker, L.D.,
6 Meyerson, E.A., Gasse, F., van Kreveland, S., Holmgren, K., Lee-Thorp, J., Rosqvist, G., Rack,
7 F., Staubwasser, M., Schneider, R.R., and Steig, E.J.: Holocene climate variability.
8 *Quaternary Res.*, 62, 243-255, 2004.

9 Mathis, M., Sorrel, P., Klotz, S., Huang, X., and Oberhänsli, H.: Regional vegetation patterns
10 at lake Son Kul reveal Holocene climatic variability in central Tien Shan (Kyrgyzstan, Central
11 Asia), *Quaternary Sci. Rev.*, 89: 169-185, 2014.

12 Miehe, G., Winiger, M., Böhner, J., and Yili, Z.: Climatic diagram map of high Asia. Purpose
13 and concepts, *Erdkunde*, 55, 94-97, 2001.

14 Mischke, S., Rajabov, I., Mustaeva, N., Zhang, C.J., Boomer, I., Brown, E.T., Andersen, N.,
15 Myrbo, A., Ito, E., and Schudack, M.E.: Modern hydrology and late Holocene history of
16 Lake Karakul, eastern Pamirs (Tajikistan): A reconnaissance study, *Palaeogeog. Palaeoclim.*
17 *Palaeoecol.*, 289: 10-24, 2010.

18 Morill, C., Overpeck, J.T. and Cole, J.E., A synthesis of abrupt changes in the Asian summer
19 monsoon since the last deglaciation, *Holocene* 13, 465-476, 2003.

20 Mügler, I., Gleixner, G., Günther, F., Mäusbacher, R., Daut, G., Schütt, B., Berking, J.,
21 Schwalb, A., Schwark, L., Xu, B., Yao, T., Zhu, L., and Yi, C.: A multi-proxy approach to
22 reconstruct hydrological changes and Holocene climate development of Nam Co, Central
23 Tibet, *J. Paleolimn.*, 43, 625-648, 2010.

24 Narama, C.: Late Holocene variation of the raigorodskogo glacier and climate change in the
25 Pamir-Alai, central Asia. *Catena*, 48, 21-37, 2002a.

26 Narama, C.: Glacier variations in Central Asia during the 20th century, *J. Geogr.*, 111 (4), 486-
27 497, 2002b.

28 PAGES 2k Network.: Continental-scale temperature variability during the last two millennia.
29 *Nat. Geosci.*, 6, 339–346, doi:10.1038/ngeo1797, 2013.

30 Prins, H.B.A., and Elzenga, J.T.M.: Bicarbonate utilization: function and mechanism. *Aquat.*
31 *Bot.*, 34, 59-83, 1989.

1 Rach, O., Brauer, A., Wilkes, H., and Sachse, D.: Delayed hydrological response to
2 Greenland cooling at the onset of the Younger Dryas in western Europe, *Nat. Geosci.*, 7, 109-
3 112, doi:10.1038/ngeo2053, 2014.

4 Rayner, N. A., D. E. Parker, E. B. Horton, C. K. Folland, L. V. Alexander, D. P. Rowell, E. C.
5 Kent, and Kaplan, A.: Global analyses of sea surface temperature, sea ice, and night marine
6 air temperature since the late nineteenth century, *J. Geophys. Res.*, 108, 4407,
7 doi:10.1029/2002JD002670, 2003.

8 Reimer, P. J., M. G. L. Baillie, E. Bard, A. Bayliss, J. W. Beck, P. G. Blackwell, C. B.
9 Ramsey, C. E. Buck, G. S. Burr, and Edwards, R.L.E.: IntCal09 and Marine09 radiocarbon
10 age calibration curves, 0-50,000 years cal BP, *Radiocarbon*, 51(4), 1111-1150, 2009.

11 Rhodes, T.E., Gasse, F., Lin, R., Fontes, J.C., Wei, K., Bertrand, P., Gilbert, E., Mélières, F.,
12 Tucholka, P., and Cheng, Z.Y.: A late pleistocene-Holocene lacustrine record from Lake
13 Manas, Zunggar (northern Xinjiang, western China), *Palaeogeog., Palaeoclim., Palaeoecol.*
14 120, 105-121, 1996.

15 Ricketts, R.D., Johnson, T.C., Brown, E.T., Rasmussen, K.A., Romanovsky, V.V.:
16 Holocene, paleolimnology of Lake Issyk-Kul, Kyrgyzstan: Trace element and stable isotope
17 composition of ostracodes, *Palaeogeog. Palaeoclim. Palaeoecol.*, 176, 207-227, 2001.

18 Risi, C., S. Bony, F. Vimeux, and Jouzel, J.: Water-stable isotopes in the LMDZ4 general
19 circulation model: Model evaluation for present-day and past climates and applications to
20 climatic interpretations of tropical isotopic records, *J. Geophys. Res.*, 115, D12118,
21 doi:10.1029/2009JD013255, 2010.

22 Risi, C., Noone, D., Worden, J., Frankenberg, C., Stiller, G., Kiefer, M., Funke, B., Walker,
23 K., Bernath, P., Schneider, M., Wunch, D., Sherlock, V., Deutscher, N., Griffith, D.,
24 Wennberg, P.O., Strong, K., Smale, D., Mahieu, E., Barthlott, S., Hase, F., García, O.,
25 Notholt, J., Wameke, T., Toon, G., Sayres, D., Bony, S., Lee, J., Brown, D., Uemura, R., and
26 Sturm, C.: Process-evaluation of tropospheric humidity simulated by general circulation
27 models using water vapor isotopologues: 1. Comparison between models and observations, *J.*
28 *Geophys. Res.*, 117, D05303, doi:10.1029/2011JD016621, 2012a.

29 Risi, C., Noone, D., Worden, J., Frankenberg, C., Stiller, G., Kiefer, M., Funke, B., Walker,
30 K., Bernath, P., Schneider, M., Bony, S., Lee, J., Brown, D., and Sturm, C.: Process-
31 evaluation of tropospheric humidity simulated by general circulation models using water
32 vapor isotopic observations: 2. Using isotopic diagnostics to understand the mid and upper

1 tropospheric moist bias in the tropics and subtropics, *J. Geophys. Res.*, 117, D05304,
2 doi:10.1029/2011JD016623, 2012b.

3 Sachse, D., Billault, I., Bowen, G.J., Chikaraishi, Y., Dawson, T.E., Feakins, S.J., Freeman,
4 K.H., Magill, C.R., McInerney, F.A., van der Meer, M.T.J., Polissar, P., Robins, R.J., Sachs,
5 J.P., Schmidt, H.-L., Sessions, A.L., White, J.W.C., West, J.B., and Kahmen, A.: Molecular
6 paleohydrology: Interpreting the hydrogen-isotopic composition of lipid biomarkers from
7 photosynthesizing organisms, *Annu. Rev. Earth Pl. Sci.*, 40, 221-249, 2012.

8 Sage, R.F., Kocacinar, F., Kubien, D.S.: C₄ photosynthesis and temperature, in: C₄
9 Photosynthesis and Related CO₂ Concentrating, *Advances in Photosynthesis and Respiration*
10 *Mechanisms*, 32, Springer Netherlands, doi: 10.1007/978-90-481-9407-0_10, 161-195, 2011

11 Schefuss, E., Schouten, S., and Schneider, R.: Climatic controls on central African hydrology
12 during the past 20,000 years, *Nature*, 473, 1003-1006, 2005.

13 Sessions, A.L., Burgoyne, T.W., and Hayes, J.M.: Correction of H₃ contributions in hydrogen
14 isotope ratio monitoring mass spectrometry, *Anal. Chem.*, 73, 192-199, 2001.

15 Seong, Y.B., Owen, L.A., Yi, C., and Finkel, R.C.: Quaternary glaciation of Muztag Ata and
16 Kongur Shan: Evidence for glacier response to rapid climate changes throughout the Late
17 Glacial and Holocene in westernmost Tibet, *Geol. Soc. Am. Bull.*, 121, 348-365, 2009a

18 Seong, Y.B., Owen, L.A., Yi, C.L., Finkel, R.C. and Schoehnbohm, L.: Geomorphology of
19 anomalously high glaciated mountains at the northwestern end of Tibet: Muztag Ata and
20 Kongur Shan, *Geomorphology*, 103, 227-250, 2009b.

21 Seth, A., Rauscher, S.A., Rojas, M., Giannini, A., and Camargo, S.J.: Enhanced spring
22 convective barrier for monsoons in a warmer world? A letter, *Climatic Change*, 104, 403-414,
23 2011.

24 Smith F. A. and Freeman K. H.: Influence of physiology and climate on δD of leaf wax *n*-
25 alkanes from C₃ and C₄-grasses, *Geochim. Cosmochimic. Ac.*, 70, 1172-1187, 2006.

26 Sorrel, P., Popescu, S.M., Klotz, S., Suc, J.P., and Oberhänsli, H.: Climate variability in the
27 Aral Sea basin (Central Asia) during the late Holocene based on vegetation changes,
28 *Quaternary Res.*, 67, 357-370, 2007a.

29 Sorrel, P., Oberhänsli, H., Boroffka, N., Nourgaliev, D., Dulski, P., and Röhl, U.: Control of
30 wind strength and frequency in the Aral Sea basin during the late Holocene, *Quaternary Res.*,
31 67, 371-382, 2007b.

1 Syed, F.S., Giorgi, F., Pal, J.S., and Keay, K.: Regional climate model simulation of winter
2 climate over Central-Southwest Asia, with emphasis on NAO and ENSO effects, *Int. J.*
3 *Climatol.*,30, 220-235, 2010.

4 Syed, F.S.: On the intra-seasonal to decadal climate variability over South-Asia, Dissertation,
5 Department of Meteorology, Stockholm University, Sweden, 2011.

6 Tian, L., Yao, T., Li, Z., MacClune, K., Wu, G., Xu, B., Li, Y., Lu, A., and Shen, Y.: Recent
7 rapid warming trend revealed from the isotopic record in Muztagata ice core, eastern Pamirs,
8 *J. Geophys. Res.*, 111, D13103, doi:10.1029/2005JD006249, 2006

9 Tierney, J.E., Russell, J.M., Huang, Y.S., Sinninghe Damsté, J.S., Hopmans, E.C., and Cohen,
10 A.S.: Northern hemisphere controls on tropical southeast African climate during the past
11 60,000 years, *Science*, 322, 252-255, 2008.

12 Thompson, L.G.: Ice core evidence for climate change in the Tropics: Implications for our
13 future, *Quaternary Sci. Rev.*, 19, 19-35, 2000.

14 Thompson, L.G., Yao, T., Davis, M.E., Henderson, K.A., Mosley-Thompson, E., Lin, P.-N.,
15 Beer, J., Synal, H.A., Cole-Dai, J., and Bolzan, J.F.: Tropical climate instability: The last
16 glacial cycle from a Qinghai-Tibetan ice core, *Science*, 276, 1821-1825, 1997.

17 Treydte, K.S., Schleser, G.H., Helle, G., Frank, D.C., Winiger, M, Haug, G., and Esper, J.:
18 The twentieth century was the wettest period in northern Pakistan over the past millennium,
19 *Nature*, 440, 1179-1182, 2006.

20 Trouet, V., Esper, J., Graham, N.E., Baker, A., Scourse, J.D., and Frank, D.C.: Persistent
21 positive North Atlantic Oscillation mode dominated the Medieval Climate Anomaly, *Science*,
22 324(78), 78-80, 2009.

23 Uppala, S. M., Kållberg, P. W., Simmons, A. J., Andrae, U., Bechtold, V. D. C., Fiorino, M.,
24 Gibson, J. K., Haseler, J., Hernandez, A., Kelly, G. A., Li, X., Onogi, K., Saarinen, S., Sokka,
25 N., Allan, R. P., Andersson, E., Arpe, K., Balmaseda, M. A., Beljaars, A. C. M., Berg, L. V.
26 D., Bidlot, J., Bormann, N., Caires, S., Chevallier, F., Dethof, A., Dragosavac, M., Fisher, M.,
27 Fuentes, M., Hagemann, S., Hólm, E., Hoskins, B. J., Isaksen, L., Janssen, P. A. E. M., Jenne,
28 R., McNally, A. P., Mahfouf, J.-F., Morcrette, J.-J., Rayner, N. A., Saunders, R. W., Simon,
29 P., Sterl, A., Trenberth, K. E., Untch, A., Vasiljevic, D., Viterbo, P. and Woollen, J.: The
30 ERA-40 re-analysis. *Q.J.R. Meteorol. Soc.*, 131, 2961-3012, 2005.

1 Wang, Z., and Liu, W.: Carbon chain length distribution in *n*-alkyl lipids: A process for
2 evaluating source inputs to Lake Qinghai, *Org. Geochem.*, 50, 36-43, 2012.

3 Wu, G.J., Yao, T.D., Xu, B.Q., Tian, L.D., Li, Z., and Duan, K.Q.: Seasonal variations of dust
4 record in the Muztagata ice cores, *Chinese Sci. Bull.*, 53 (16) 2506-2512, 2008.

5 Wünnemann, B. , Demske, D. , Tarasov, P. , Kotlia, B. S. , Reinhardt, C. , Bloemendal, J. ,
6 Diekmann, B. , Hartmann, K. , Krois, J. , Riedel, F. and Arya, N.: Hydrological evolution
7 during the last 15 kyr in the Tso Kar lake basin (Ladakh, India), derived from
8 geomorphological, sedimentological and palynological records, *Quaternary Sci. Rev.*, 29,
9 1138-1155, 2010.

10 Wünnemann, B., Mischke, S., and Chen, F.: A Holocene sedimentary record from Bosten
11 Lake, China. *Palaeogeog. Palaeoclim. Palaeoecol.*, 234: 223-238, 2006.

12 Yao, T., Thompson, L., Yang, W., Yu, W., Gao, Y., Guo, X., Yang, X., Duan, K., Zhao, H.,
13 Xu, B., Pu, J., Lu, A., Xiang, Y., Kattel, D.B., and Joswiak, D.: Different glacier status with
14 atmospheric circulations in Tibetan Plateau and surroundings, *Nat. Clim. Change*, 2, 663-667,
15 2012.

16 Yao, T., Masson-Delmotte, V., Gao, J., Yu, W., Yang, X., Risi, C., Sturm, C., Werner, M.,
17 Zhao, H., He, Y., Ren, W., Tian, L., Shi, C., and Hou, S.: A review of climatic controls on
18 $\delta^{18}\text{O}$ in precipitation over the Tibetan Plateau: Observations and simulations, *Rev. Geophys.*,
19 51, 525-548, 2013

20 Zhang, X., and Cong, Z.: Trends of precipitation intensity and frequency in hydrological
21 regions of China from 1956 to 2005, *Global Planet. Change*, 117, 40-51, 2014

22 Zhao, K., Li, X., Dodson, J., Atahan, P., Zhou, X., and Bertuch, F.: Climatic variations over
23 the last 4000 cal yr BP in the western margin of the Tarim Basin, Xinjiang, reconstructed
24 from pollen data, *Palaeogeog. Palaeoclim. Palaeoecol.*, 321-322: 16-23, 2012.

25 Zhong, W., Xue, J. B., Shu, Q. and Wang, L. G.: Climatic change during the last 4000 years
26 in the southern Tarim Basin, Xinjiang, northwest China. *J. Quaternary Sci.*, 22, 659-665, 2007

27 Table 1: $\delta^{18}\text{O}$ and δD values of water samples collected in September 2008 at Lake Karakuli,
28 its inflows and nearby ponds.

29
30
31
32

1 **Tables**

2

3 Table 1: $\delta^{18}\text{O}$ and δD values of water samples collected in September 2008 at Lake Karakuli,
4 its inflows and nearby ponds.

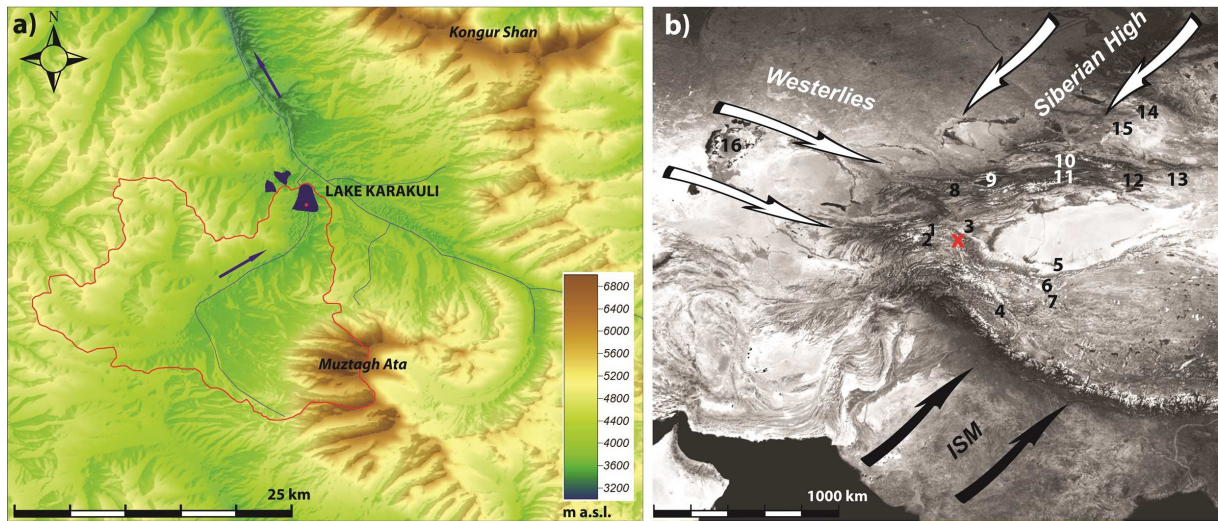
5

6

Latitude [°N]	Longitude [°E]	Altitude [m]	Description	$\delta^{18}\text{O}$ [‰]	1 σ	δD [‰]	1 σ
38.41933	75.05995	3684	inflow1	-12.1	0.05	-83.2	0.2
38.42021	75.05008	3688	inflow2	-12.1	0.01	-84.4	0.2
38.43968	75.05725	3657	Karakuli - core position surface water	-9.4	0.04	-67.8	0.2
38.43968	75.05725	3657	Karakuli - core position above sediment	-9.2	0.03	-67.2	0.2
38.46294	75.02928	3658	pond near Karakuli	5.45	0.02	13.5	0.4
38.46334	75.04267	3676	pond near Karakuli	-3.6	0.02	-37.1	0.5

7

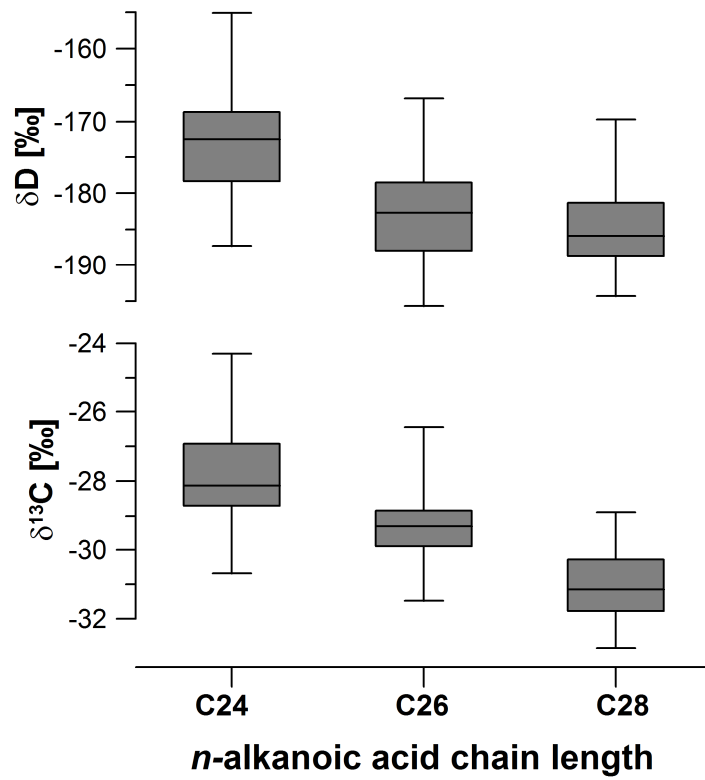
1 **Figures**



2
3

4 Fig. 1: (a) Catchment of Lake Karakuli and coring position (red dot). (b) Location of our
5 study area (red cross) and other paleoclimatic records mentioned in the text. 1: large Lake
6 Karakul, Tajikistan (Mischke et al., 2010); 2: Lake Sasi Kul (Lei et al., 2014); 3: Kashgar
7 (Zhao et al., 2012); 4: Tso Kar (Wünnemann et al., 2010); 5: Southern Tarim Basin (Zhong et
8 al., 2007); 6: Guliya Ice Core (e.g. Thompson et al., 1997); 7: Lake Bangong (Gasse et al.,
9 1996); 8: Son Kol (Lauterbach et al., 2014, Mathis et al., 2014), 9: Issyk Kul (Ricketts et al.,
10 2001); 10: Yili section (Li et al., 2011); 11: Kesang Cave (Cheng et al., 2012); 12: Boston Hu
11 (Wünnemann et al., 2006); 13: Lake Balinkun (An et al., 2012); 14: Ulungur Hu (Liu et al.,
12 2008); 15: Lake Manas (Rhodes et al., 1996); 16: Aral Sea (Sorrell et al., 2007a and b;
13 Boomer et al., 2009; Huang et al., 2011).

14

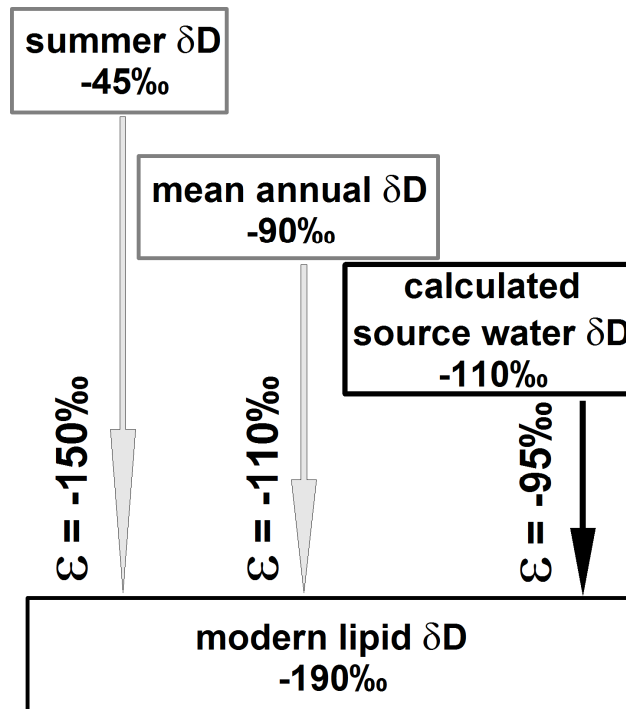


1

2

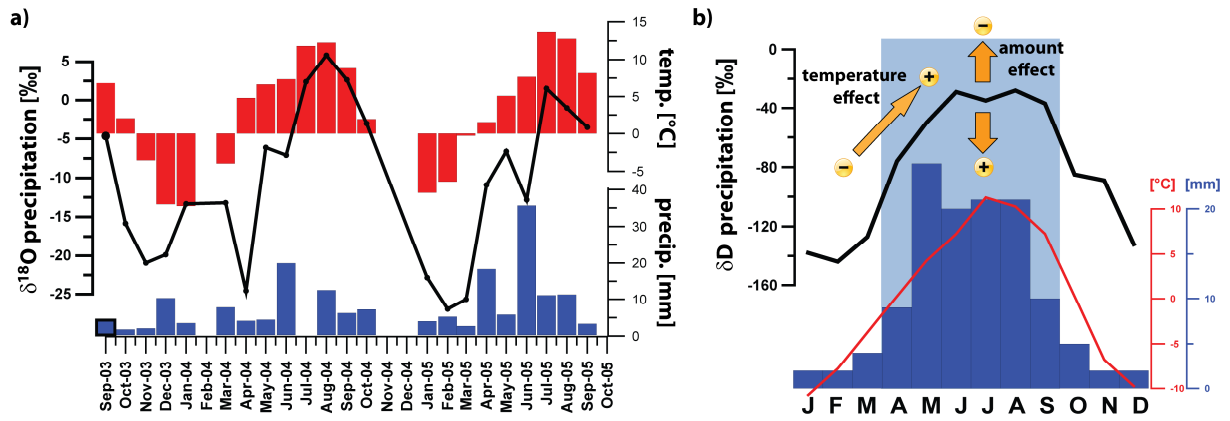
3 Fig. 2: Box and whisker plots of δD and $\delta^{13}C$ values in sediment samples by chain length.

4



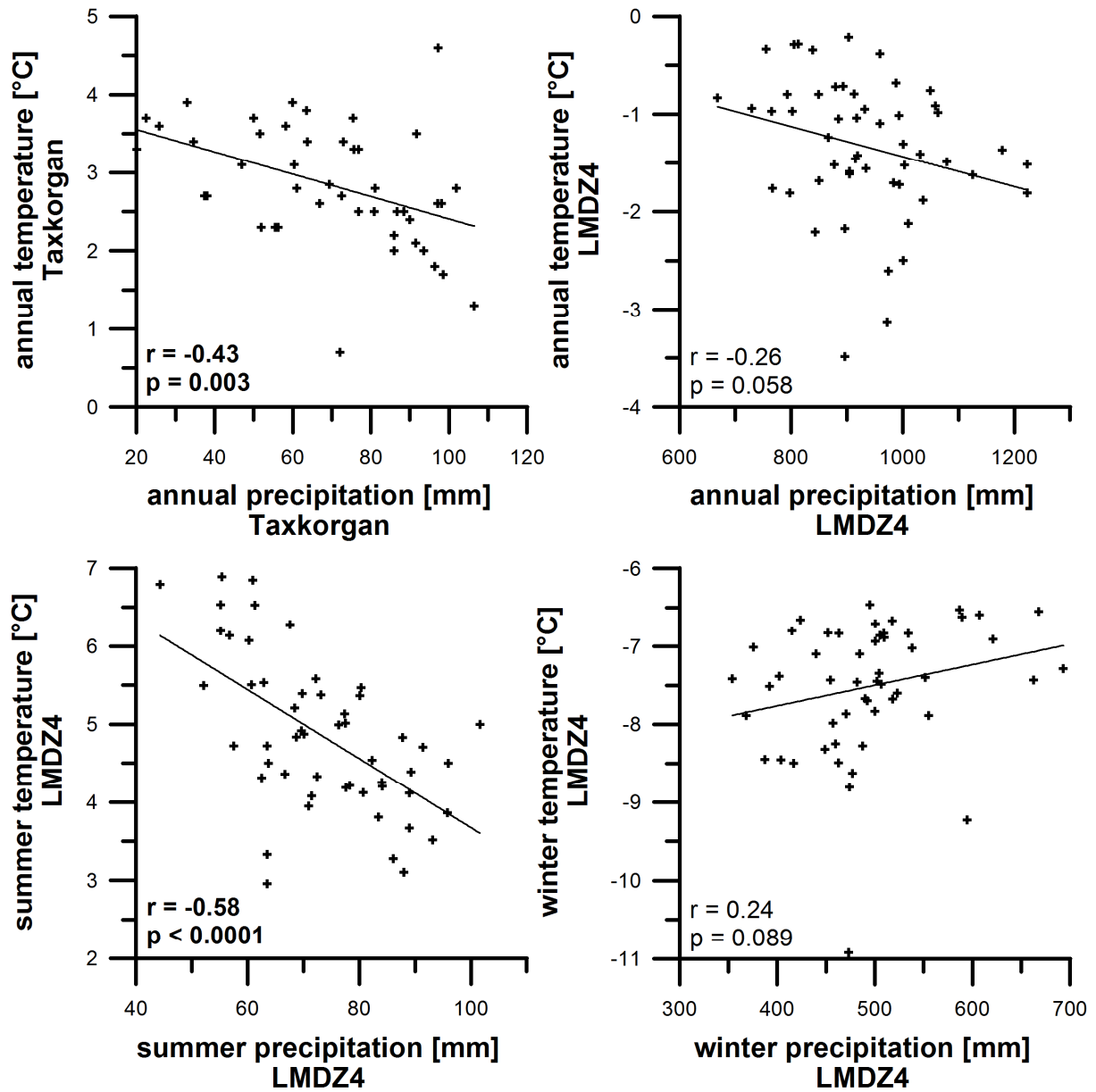
1
2
3
4
5
6
7

Fig. 3: Calculated isotopic fractionation factors (ϵ) between summer and mean annual precipitation and modern lipids, as well as calculated source water δD on basis of published fractionation factors in arid ecosystems (ca. -95‰ according to Feakins and Sessions, 2010; Günther et al., 2013).



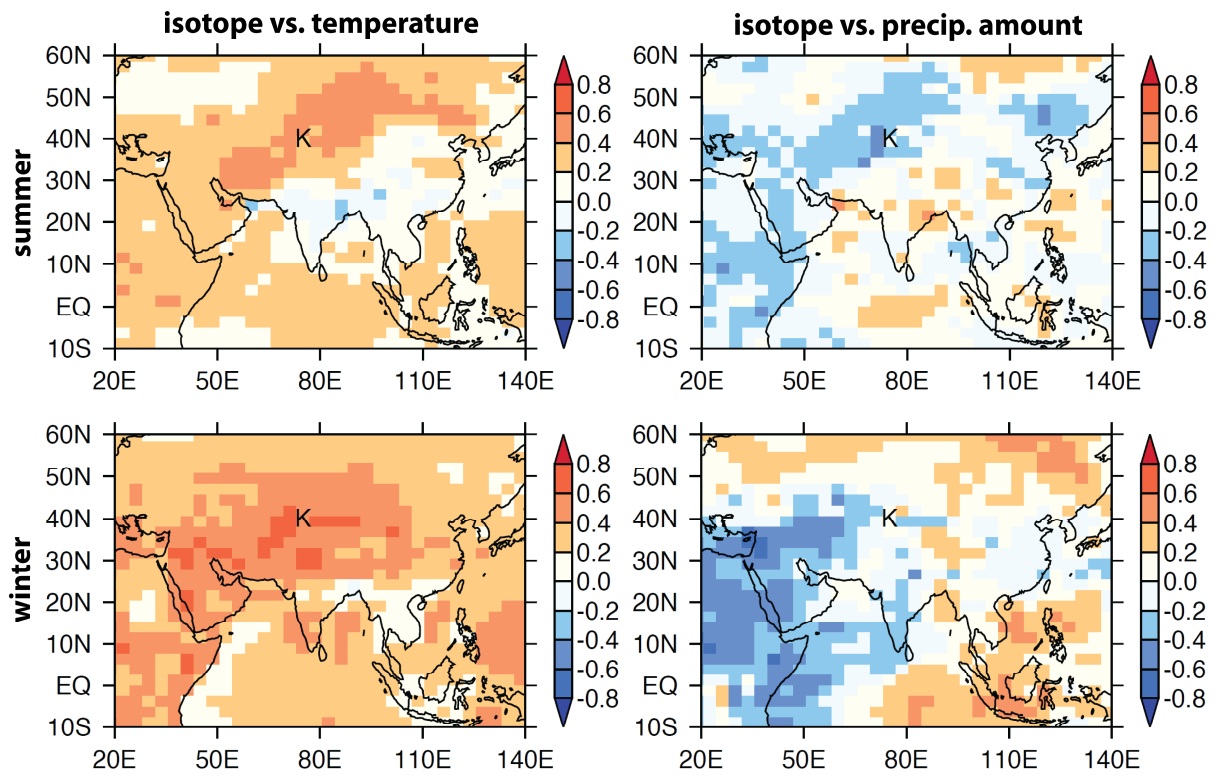
1
2
3
4
5
6
7

Fig.4: (a) Monthly isotopic and climate data from Taxkorgan climate station (Yao et al., 2013), located ca. 80 km south of Lake Karakuli (altitude ca. 3100 m). (b) Average monthly climate (Miehe et al., 2001) and isotopic (OIPC; Bowen and Revenaugh, 2003) data from Bulun Kul climate station located ca. 30 km northeast of Lake Karakuli (altitude ca. 3300 m). Shaded area indicates summer/wet season.

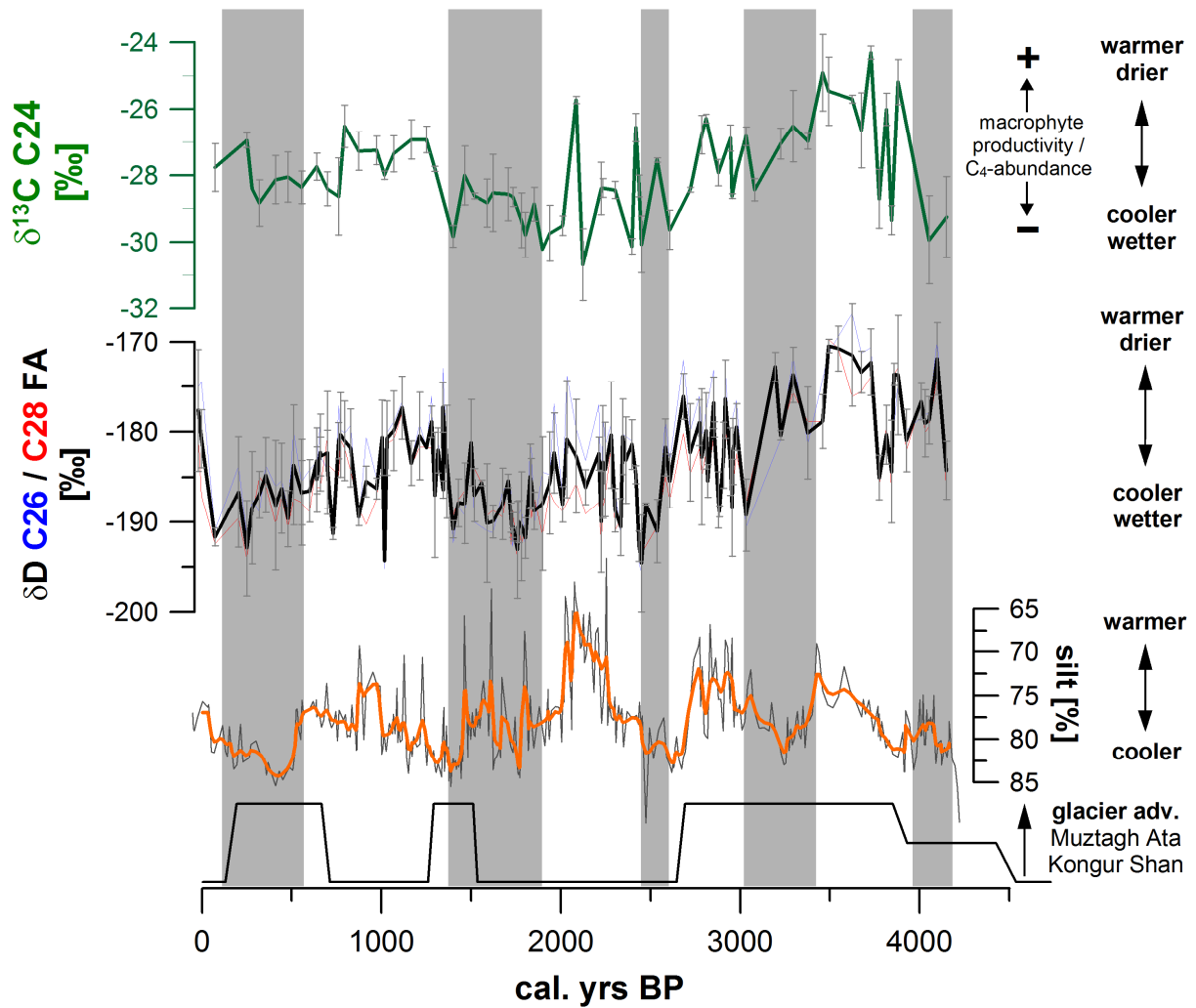


1
 2 Fig. 5: Correlations of temperatures with precipitation amounts based on instrumental data
 3 from Taxkorgan meteorological station (1957-2000; annual averages) and model data using
 4 LMDZ4 simulations (1958-2009; summer: April-September; winter: October-March). Bold
 5 correlation coefficients are significant at the 0.01-level.

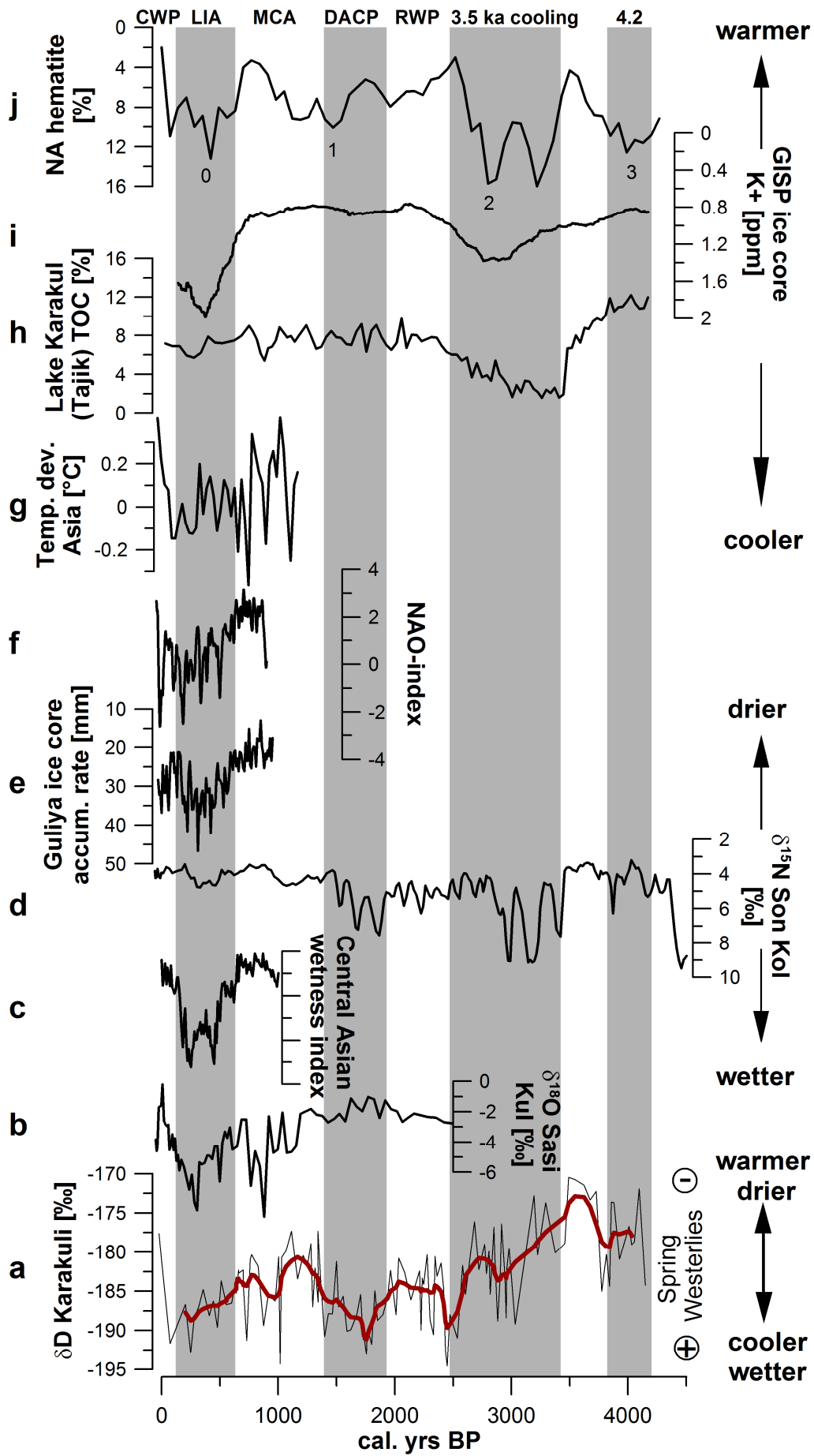
6



1
 2 Fig. 6: Spatial correlation coefficient (r) summer (April-September) and winter (October-
 3 March) $\delta^{18}\text{O}$ of precipitation at the Karakuli site (marked as K in the plots) with temperatures
 4 and precipitation amounts at each grid point from 1958 to 2009 using LMDZ4 simulations
 5 (Lee et al., 2012).



1
 2 Fig. 7: Summary of organic geochemical results from this study in context with silt contents
 3 of the same sediment core (Liu et al., 2014; orange line: 5-point weighted average) and data of
 4 local glacier advances on basis of ^{10}Be -dating (Seong et al., 2009a; centers and widths of
 5 boxes mark the mean age and the error ranges of the events). Biomarker hydrogen isotopic
 6 data are presented as mean of triplicate measurements for the C₂₆ (blue line) and C₂₈ *n*-
 7 alkanolic acids (red line) as well as unweighted average of the two (thick black line, with 1σ
 8 error bars). Shaded areas are relatively cool and wet episodes, based on leaf wax isotopic data.



1 Fig. 8: Comparison to local and Northern Hemispheric paleorecords. Shaded areas indicate
2 relatively cool/wet episodes at Lake Karakuli; (a) δD of C_{26} and C_{28} *n*-alkanoic acids Lake
3 Karakuli (this study); average values as in Fig. 8, red line: 5-point weighted average. (b) $\delta^{18}O$
4 Sasi Kul, Pamir, Tajikistan (Lei et al., 2014). (c) Central Asian wetness index (Chen et al.,
5 2010). (d) $\delta^{15}N$ TN, Son Kol, Central Tien Shan, Kyrgyzstan (Lauterbach et al., 2014). (e)
6 Guliya ice core accumulation rate (Thompson et al., 1997). (f) North Atlantic Oscillation
7 index (Trouet et al., 2009). (g) 30-year average of compiled temperature deviations in Asia
8 (Pages 2k Network, 2013). (h) TOC-contents large Lake Karakul, Pamir, Tajikistan (Mischke
9 et al., 2010). (i) K^+ GISP2 ice core (Mayewski et al., 1997). (j) Northern Atlantic Hematite
10 grains indicate Northern Hemispheric cooling events “Bond-events” (Bond et al., 2001).

11